Effect of High Magnetic Field on a Quasi-3D Silver Dendrite Growing System

Fengzhi Tang[1†], Akio Katsuki[2]*, Yoshifumi Tanimoto[1]*

[1]Graduate School of Science, Hiroshima University, Higashi-Hiroshima 739-8526, Japan

[2]Department of Chemistry, Faculty of Education, Shinshu University, 6-Ro, Nishi-Nagano, Nagano 380-8544, Japan

[†]Fengzhi Tang was a Hiroshima University Study Abroad student from Huazhong University of Science & Technology.

Authors for corresponding,

Akio Katsuki

Fax: +81 26 238 4123

e-mail: akatuki@ shinshu-u.ac.jp

Yoshifumi Tanimoto

Fax: +81-82-424-7409

e-mail: tanimoto@sci.hiroshima-u.ac.jp

Abstract

The Ag^+/Cu liquid-solid redox reaction was investigated in a vertical and inhomogeneous high magnetic field (up to 15 T). According to a comparison between morphologies of quasi-3D silver dendrites generated under different magnetic flux densities, the imposition of a high magnetic field strongly affected the silver dendrites' aggregation process. The present experiment used four kinds of liquid-solid boundaries, which are affected by the reaction direction and a solution condition, as bases for silver depositions' diffusion limited aggregation (DLA)-like dendritic growth. Results are interpreted in terms of convections of the aqueous solution and a tentative quantitative analysis of forces acting on particles arising from the magnetic field. Moreover, a new force is predicted theoretically and is discussed in detail.

1. Introduction

In the early 1980s, diffusion limited aggregation (DLA) was first proposed and simulated by Witten and Sander [1, 2]. In nature, DLA-like growth is ubiquitous from electrodeposited metals to newly formed river basins, from bacterial colonies to blood vessels in the eye, and in the initial stages of urban sprawl. Since then, non-equilibrium and irreversible aggregations have been examined using numerous computer simulations and experiments [3-19]. Myriad parameters were revealed to influence morphologic properties of aggregation, both by computational methods and experimental methods. Using former methods such as particle drift [4], strength and direction of flow [5, 6, 9], the shape of depositional boundary [7], growth velocity [8], convection [9], interfacial instability, and noise were found [10]. Those experimental methods are complementary and indispensable. Moreover, by observation, other parameters such as solution concentration, species of metallic deposition [11-16] and crystalline anisotropy and supersaturation [19] were also revealed as important, along with computational results confirmed in real reaction systems. In short, the pattern of aggregates depends strongly upon growth-process dynamics.

A high magnetic field is a useful tool to investigate aggregation processes in experiments because it is convenient to apply and it can alter various parameters as mentioned above. Mogi et al. carried out a series of redox reactions to investigate 2-dimensional (2D) dendrite patterns using a vertical and homogeneous high magnetic field. Those studies concluded that magnetohydrodynamism (MHD) induces convection and lateral drift; thereby, it affects the geometric properties of the patterns [11-16].

Kozuka et al. reported that a micro-MHD effect, magnetization force, and magnetic convection strongly influence metal substitution reactions under an intense magnetic field [25]. Our group also studied the magnetic field effect (MFE) of vertical and horizontal inhomogeneous high magnetic fields on chemical reactions. Tanimoto et al. demonstrated the MFE on the yield of metal deposition and orientation of different species of 2D metal dendrites in a horizontal field [23]. Duan et al. confirmed that assumption through the use of computer simulations [24]. Katsuki investigated MFE on 2D and 3D silver dendrites in a vertical field [20-22]. Furthermore, Uechi et al. reported that MFE determined 3D-morphological chirality, along with some other properties of silicate membrane tubes from a silicate garden reaction [26, 27]. Therefore, a magnetic field can be considered as a pattern ‘tailor’. But how does this tailor actually operate, especially when using microscopic and quantitative analyses, which are necessary?

In this study, through application of a vertical inhomogeneous high magnetic field, the morphologic change of silver dendrites grown from four kinds of boundaries in a quasi-3D system is explained via the change of the growth rate, Lorentz force (MHD force), and convection influence based on the precursors’ concentrations. The boundary conditions depend on whether a reaction direction of the silver ions is inner or outer, and whether the silver ions in a solution are able to react toward both directions (the common solution) or one direction (separated solution). Finally, the results are analyzed specifically and quantitatively in a diffusion layer model to examine and compare the forces that act on particles.

2. Experimental

Figure 1 shows two kinds of experimental setup. In set-up (I), an annular pure copper plate (11.60 mm inner diameter, 17.70 mm outer diameter, 0.25 mm thickness) was used. Both inner and outer boundaries of the plate were treated as bases for growing silver dendrites. In set-up (II), a circular pure copper plate (4.70 mm diameter, 0.25 mm thickness) and an annular pure copper plate (19.70 mm inner diameter, 29.70 mm outer diameter, 0.25 mm thickness) were used: the circular plate's outer boundary and the annular plate's inner boundary were treated as bases. Copper plates were pre-cleaned using an acidic cleansing agent and then pasted and fixed in the centre of the bottom of a cylindrical glass vessel (32.30 mm diameter, 19.10 mm depth; flat bottom). After an appropriate amount of silver nitrate aqueous solution (0.020 mol/dm^3 for set-up (I), 0.025 mol/dm^3 for set-up (II)) was added to the vessel, another circular glass plate (29.75 mm diameter, 2.60 mm thickness, with a 2.50 mm diameter hole in the centre) was used to cover the upper surface of copper plates to restrict the Ag^+/Cu liquid-solid redox reaction occurring only at the boundaries of copper plates. The thickness of the reacting layer nearly equalled the copper plate thickness: 0.25 mm. The experiments with high magnetic fields were carried out in a bore tube (40 mm diameter) of a superconducting magnet (JMTD-LH15T40; Japan Superconductor Technology, Inc.). The distribution of the magnetic field and the magnetic field gradient are displayed in Fig. 2. Reactions occurred under 4 T, 6 T, 9 T, 12 T, and 15 T downward magnetic fields by placing the reacting cell at different heights of the bore. Another experiment was carried out outside as a control reaction, where the magnetic flux density and field gradient were so small (ca. 5 mT) as to be negligible. The reactive time for set-up (I) was 1 h, but 1.5 h for set-up (II); all experiments were carried out at room temperature (ca. 25°C). After reaction, the silver dendrite patterns were recorded using a digital camera.

3. Results

The in situ redox reaction, as shown in the following chemical equation, is rather simple:

$$Cu + 2Ag^{+} \rightarrow 2Ag\downarrow + Cu^{2+}. \quad (1)$$

Because of the different redox potentials of Cu/Cu^{2+} and Ag/Ag^{+}, this reaction occurs spontaneously.

Figure 3 and Fig. 4 show silver dendrite patterns in the two set-ups. The silver dendrite patterns were affected strongly by the imposed high magnetic field. Moreover, with the increasing magnetic flux density, the patterns exhibited a regular tilting tendency, especially in set-up (II).

As shown in pattern Fig. 3(a) and Fig. 4(a), outside, the morphology displayed a typical and symmetrical DLA-like pattern. An open-ramified pattern (a spread-pattern of the branches) was generated with small dendrites between big ones, as reported by Witten [1, 2]. It showed good agreement with Mogi's experiments [11] and with many DLA-like patterns created by computer simulations.

In the 4 T magnetic field, the pattern changed to a dense branching morphology: the dendrites seem to have uniform size and no large ramifications (spread of their branches). The distance separating the adjacent main dendrites decreased along with the dendrite widths, whereas the number of dendrites increased. Moreover, the dendrites grown from all the boundaries formed a smooth circular periphery. In addition, the silver dendrites grown from the inner boundary of set-up (I) and the outer boundary of set-up (II) inclined counterclockwise, while those from the outer boundary of set-up (I) and the inner boundary of set-up (II) slanted clockwise.

In subsequently higher magnetic fields, different dendrite patterns emerged for the two set-ups. In set-up (I), the pattern became extremely dense and compact. However, in set-up (II), the dendrite length shortened concomitant with the increasing magnetic field. The number of dendrites increased from the 4 T condition to 12 T condition, whereas the tilting of dendrites was only slightly observable with or without order under magnetic field above 6 T. Nonetheless, in both set-ups, the dendrites colour darkened as the magnetic flux density increased, from which it is readily inferred that the dendrites' density and thickness were enhanced. It is strange that the number of the main dendrites decreased suddenly according to the photographs shown in Figs. 4(c) and 4(d); the dendrites became non-uniform again.

4. Discussion

4.1 Explanation of morphologic change

First, the DLA pattern is explainable by the random walk model of a diffusion system [1-3]. Generally, the electron transfer process of the present redox reaction is much faster than the diffusive mass-transfer process of silver ions [11]. Consequently, the growth rate of a point depends on the effective rate of diffusive transport in its neighbourhood. The arms of large dendrites can shield the adjacent inner portions. Therefore, the subsequent silver particles attach to protuberances. Because the small dendrites are thereby screened, the larger ones mainly grow and ramify haphazardly.

After imposing a high magnetic field, the initial condition should be modified. The MHD effect is applicable. Numerous and various ions exist, such as Cu^{2+}, Ag^{+}, NO_3^{-} and so on. These ions are undergoing continuous movements such as thermodynamic motion and beamed diffusive motion. The magnetic field is applied vertically downward in the present experiment. Hence, Lorentz force gives torque to any horizontal ionic movement, based on the following well-known equation:

$$\boldsymbol{F}_L = q\boldsymbol{v} \times \boldsymbol{B} , \qquad (2)$$

where q is the charge of an ion, $\boldsymbol{v}$ is its velocity, and $\boldsymbol{B}$ is the magnetic flux density. Accordingly, the solution is stirred. Especially, near the interface between the copper boundaries and the silver nitrate solution, a beamed diffusive motion of Ag^{+} ions extends from the bulky solution to the interface, so an oriented convection of Ag^{+} ions occurs. However, the trajectory of the Ag^{+} ions shifts depends on the condition of the boundary. In the present experiment, four kinds of boundaries exist, which are used to confirm this mechanism. Based on Eq. (2), in the present experiment, the Ag^+ ions that move from the edge to the centre part of vessel feel a counterclockwise torque. In contrast, the Ag^+ ions move along the opposite direction feel a clockwise torque, which can explain the orientation of the dendrites grown from different boundaries. This mechanism is shown schematically in Fig. 5.

The MHD inducing flow can stir the solution and produce perturbations that can consequently shorten the diffusion length of silver ions and reduce the screen effect [11, 16]. Thus, the DLA-like pattern becomes a dense-branching morphology in a magnetic field.

Differences of patterns between set-up (I) and set-up (II) are that, in the case of set-up (II), only a small amount of solution confined between the copper plates can react as the source of silver dendrites. However, in the case of set-up (I), all of the solution in the vessel can react with the copper. Therefore, the dendrites in set-up (I) are much denser and more compact than that in set-up (II).

The sequential change of the dendrites' colour and the change of distance between adjacent main dendrites occur because the reaction rate is enhanced with the increasing magnetic field. The MHD induced flows and perturbation can accelerate the diffusive process of silver ion [11, 20, 23]. Kozuka et al. reported that the microscopic Lorentz force can promote the reaction rate according to the interaction between the current loops and the magnetic field [25]. Moreover, the magnetic-force-induced convection can also promote the reaction rate, as described more specifically in next section. Because of the enhanced reaction rate, the number of dendrites also increases and the pattern becomes denser and more compact. For set-up (II), because the amount of silver ions that can generate dendrites is limited, whereas the dendrites becomes denser and numerous, the dendrite length should become shorter.

A plausible explanation for the sudden change of the dendrite number under 15 T magnetic field is as follows: no magnetic gradient pertains in this condition, so the magnetic force induced convection does not exist, which can strongly weaken the diffusive process of silver ion. Moreover, the magnetic flux density is extremely high, which might cause the randomly moving ions that perform random roll convection attributable to the extremely strong Lorentz force. In this condition, roll convection is the dominating effect on dendritic growth. This assumption is in good agreement with Nagatani's computer simulation of thermal convection, which can be considered as a random roll convection of particles [9].

The dendrites under a high magnetic field (above 6T) did not incline visibly, as mentioned above. Partly, it is because that the dendrites in that condition were relatively short, which makes them hard to observe.

4.2 Quantitative analysis of forces acting on particles

In the present experiment, it is unreasonable that the dendrites did not incline much under the relatively high magnetic field if we consider this question only via the MHD mechanism. The reason is that, with increasing magnetic flux density, the later drift of silver ions should become larger, based on Eq. (2). We must reformulate the model in terms of quantitative analysis of forces acting on particles to resolve this apparent contradiction. A new force was induced by the interaction between the magnetic field and the concentration gradient of the electrolytic solution.

Reportedly, in the magnetic field, the material energy is calculable in the following equation, as well as forces induced by the magnetic field [28].

$$E_{mag} = -\frac{1}{2}\mu_0 \chi \mathrm{H}^2 \tag{3}$$

$$F_{mag} = -gradE_{mag} \tag{4}$$

In those equations, E_{mag} is energy, μ_0 is the vacuum permeability constant, χ is the magnetic susceptibility; F_{mag} is the force induced by the magnetic field. Units depend on different calculating processes.

In the present experiment, vertically, the magnetic field has a gradient. However, horizontally, because of the reaction, a concentration gradient must exist for both the reactant (silver ion) and product (copper ion) from bulk solution to the interface surface.

$$F_{mag} = \frac{1}{2\mu_0} B^2 \frac{\partial \chi_y}{\partial y} + \frac{\chi}{\mu_0} B_z \frac{\partial B_z}{\partial z} \qquad (5)$$

In that equation, the y direction is the horizontal radial direction toward the interface between the copper and the solution, the z direction is the upward vertical direction the same as the magnetic field. The first term of the right part is the force in the horizontal radial direction because of the magnetic susceptibility gradient due to the concentration gradient along the y direction. The second term is the vertical force attributable to the field gradient. For simplicity, the former is named F_h, and the latter is named F_v in the following context.

Vertically, compared with the ion size, the copper boundary thickness (0.25 mm) is great, which also explains this system's name: Quasi-3D system. For copper ion, the direction of F_v is upward, along the positive direction of component z because of its paramagnetic property (1.97×10^{-8} m^3 mol^{-1}). For silver ions, the F_v direction is downward, along the negative direction of component z, because of its diamagnetic property (-5.87×10^{-10} m^3 mol^{-1}). For example, when the field gradient equals 200 T^2 m^{-1}, F_v and gravity is estimated as nearly 3.14 N mol^{-1} and 0.62 N mol^{-1} for copper ions, -0.093 N mol^{-1} and 1.06 N mol^{-1} for silver ions respectively via following equations.

$$F_v = \frac{\chi}{\mu_0} B_z \frac{\partial B_z}{\partial z} \tag{6}$$

$$G = mg \tag{7}$$

Especially for copper ions, even in 200 T^2 m^{-1} field gradient, F_v is more than five times gravity, other data are shown in Table 1. Therefore, F_v enhances the natural convection in the solution, which is that silver ions go downward while copper ions go upward because the silver ion density (107.9 g mol^{-1}) is greater than that of copper ion (63.55 g mol^{-1}), which is shown as Fig. 6(a). This enhanced convection is a salient reason that the reaction rate was accelerated in the magnetic field [20].

Horizontally, if a radial magnetic gradient is neglected, it can be presumed that the solution has its bulk concentration c up to a distance δ from the outer Helmholtz plane, and then falls linearly to c' at the plane itself (see Fig. 6(b)) [29]. For simplicity, only silver ions are considered. This diffusive layer is called the Nernst diffusion layer, which is well known in electrochemistry and is typically 0.1 mm [29]. Although the present reaction is not an electrode reaction but a redox reaction, the electron transfer process exists in the reaction. It is reasonable that there be a diffusive layer between the bulky solution (rich in silver ions) and the copper interface. Thus, it is reasonable to consider that this diffusive layer is similar to the Nernst layer. This layer is illustrated in Fig. 6(b).

The concentration gradient through the diffusive layer is described as

$$\frac{\partial c}{\partial y} = \frac{(c - c')}{\delta} \quad . \tag{8}$$

This gradient gives rise to a flux of silver ions towards to the interface, flux J is proportional to the concentration gradient according to Fick's Law,

$$J = -D\left(\frac{\partial c}{\partial y}\right), \tag{9}$$

where D is the diffusion coefficient. In the diffusive layer, the current density j toward the interface is

$$j = nFJ = -nFD\frac{(c - c')}{\delta}, \tag{10}$$

F is Faraday's constant, and n is the valence number.

From Ref. 30, the Lorentz force density F_L is as

$$F_L = \vec{j} \times \vec{B}, \tag{11}$$

where the unit of F_L is N m^{-3}. Also, B is the imposed magnetic flux density. According to the Nernst-Einstein equation

$$\lambda = \frac{n^2 F^2 D}{RT} \quad , \tag{12}$$

where λ is the limiting ionic conductivities in water at 25 °C. It is a constant for a certain ion. We can obtain the following equation from Eqs. (10)–(12).

$$F_L = -\frac{(c - c')RT\lambda B}{nF\delta} \tag{13}$$

Volume susceptibility χ_v can be approximated to calculate by multiplying molar susceptibility χ by the concentration of the material:

$$\chi_v = \chi c\,. \tag{14}$$

According to Eqs. (5) and (8), a horizontal magnetic force F_h is described as

$$F_h = (1/2\mu_0)B^2\chi\,(c - c')/\delta\,. \tag{15}$$

The unit of F_h is also N m^{-3}. Now we can compare F_L with F_h. The proportion is

$$\left|\frac{F_L}{F_h}\right| = \frac{(c - c')RT\lambda B}{nF\delta} \times \frac{2\mu_0\delta}{B^2\chi(c - c')} = \frac{2\mu_0 RT\lambda}{nF\chi} \times \frac{1}{B}\,. \tag{16}$$

The proportion between F_L and F_h corresponds only with the magnetic flux density because the parameters in the first term of the right part are all constants for a certain parameter in a certain condition. Consequently, it can be presumed that

$$\left|\frac{F_L}{F_h}\right| = \frac{k}{B}, \tag{17}$$

where k is a constant.

For silver ion, which influences dendritic growth directly, μ_0 is $4\pi \times 10^{-7}$ J s^2 C^{-2} m^{-1}, R is 8.314 J K^{-1} mol^{-1}, T is 298 K, n is 1, F is 9.6485×10^4 C mol^{-1}, χ is $\mu_0 \times (-4.57) \times 10^{-4}$ m^3 mol^{-1} [30, 31]. Therefore, k is calculable as 0.681 T^{-1}, presuming that only silver ions are considered. According to Eq. (17), the proportion is related to the reciprocal of the value of magnetic flux density, as shown in Fig. 7. With increasing magnetic flux density, F_L, which is the promoter of lateral drift, becomes lower than F_h, which represents the radial force. For this reason, the dendrite did not tilt markedly in the high field but inclined in a relatively low field. Because of the diamagnetic property of silver ion, according to Eq. (15), the direction of F_h is oriented to the interface, which can also enhance the silver ion transportation process and thereby accelerate the reaction rate with an increased magnetic field.

For simplicity, we can consider c' as 0: c is 0.025 mol/dm^3 at the first stage of the reaction and the thickness of the diffusion layer is 0.1 mm. Therefore, we can calculate F_L and F_h respectively according to Eq. (13) and Eq. (15), where the limiting ionic conductivity of silver ion λ is 6.19×10^{-3} S m^2 mol^{-1}. The calculation result using these parameters is shown in Fig. 7; the specific values are listed in Table 1. According to Fig. 7, the ratio of F_L to F_h is nearly one at 0.7 T, indicating that horizontal forces induced by the gradient of magnetic susceptibilities are unexpectedly important.

5. Conclusion

A magnetic field affects the dendrite growth process in terms of three kinds of forces acting on ions in different directions. Through quantitative analyses of these forces, we can elucidate which force is dominant or affects the process mainly in a certain condition. Vertically, the magnetic field gradient enhances natural convection, thereby accelerating the reaction rate. Horizontally, the radial magnetic force, which is determined in this study, combined with Lorentz force, can greatly influence the silver dendrite pattern morphology. These two forces are also an important factor to enhance the reaction rate. With increasing magnetic field, the radial force (magnetic force, F_h) becomes increasingly greater than the lateral force (Lorentz force, F_L). Consequently, the dendrites did not incline much in the high field. This approach is tentative, but, importantly, it explains phenomena quantitatively

Acknowledgment

F.T. thanks Hiroshima University Study Abroad program for scholarship. This research was partially supported by the Grant-in-Aid for Scientific Research on Priority Area “Innovative utilization of strong magnetic fields” (Area 767, Nos. 15085208 and 15085205) from MEXT of Japan, and Grant-in-Aid for Scientific Research (B), 16350007, 2004.

References

[1] Witten, T. A., and Sander, L. M., 1981, *Phys. Rev. Lett.*, **47**, 1400.

[2] Witten, T. A., and Sander, L. M., 1983, *Phys. Rev. B*, **27**, 5686.

[3] Rikvold, P. A., *Phys. Rev. A.*, 1982, **26**, 647.

[4] Meakin, P., *Phys. Rev. B.*, 1983, **28**, 5221.

[5] Nagatani, T., and Sagues, F., 1990, *J. Phys. Soc. Jpn.*, **59**, 3447.

[6] Nagatani, T., 1989, *Phys. Rev. A*, **39**, 438.

[7] Nagatani, T., and Sagues, F., 1991, *Phys. Rev. A,* **43**, 2970.

[8] Saito, Y., Uwaha, M., and Seki, S., 1992, *Pattern Formation in Complex Dissipative systems*, Ed. Kai, S. (Singapore: World Science), p. 47-56.

[9] Nagatani, T., [8], p. 83-87.

[10] Ohta, S., [8], p. 93-97.

[11] Okubo, S., Mogi, I., and Nakagawa, Y., [8], p. 98-102.

[12] Mogi, I., Okubo, S., and Nakagawa, Y., 1991, *J. Phys. Soc. Jpn.*, **60**, 3200.

[13] Mogi, I., Okubo, S., and Nakagawa, Y., *J. Crystal Growth*, 1993, **128**, 258.

[14] Mogi, I., Okubo, S., and Nakagawa, Y., 1993, *Electrochemical Processing of Tailored Materials* (2nd International Symposium), Alkire, R., Masuko, N., and Sadoway, D. R. Eds., PV 93-12, Honolulu, Hawaii, p. 136-146.

[15] Okubo, S., Mogi, I., and Kido, G., and Nakagawa. Y., 1993, *Fractals*, **1**, 425.

[16] Mogi, I., Kamiko, M., and Okubo, S., 1995, *Physica* B, **211**, 319.

[17] Miyazima, S., Maruyama, K., Okumura, K., and Oota, Y., [8], p. 79-82.

[18] Grier, D., Ben-Jacob, E., Clarke, R., and Sander, L. M., 1986, *Phys. Rev. Lett.*, **56**, 1264.

[19] Sawada, Y., Dougherty, A., and Gollub, J. P., 1986, *Phys. Rev. Lett.*, **56**, 1260.

[20] Katsuki, A., Uechi, I., and Tanimoto, Y., 2004, *Bull. Chem. Soc. Jpn.*, **77**, 275.

[21] Katsuki, A., Uechi, I., and Tanimoto, 2005, *Bull. Chem. Soc. Jpn.*, **78**, 1251.

[22] Katsuki, A., and Tanimoto, 2005, *Chem. Lett.*, **34**, 726.

[23] Tanimoto, Y., Yano, H., Watanabe, S., Katsuki, A., Duan, W., and Fujiwara, M., 2000, *Bull. Chem. Soc. Jpn.*, **73**, 867.

[24] Duan, W., Fujiwara, M., and Tanimoto, Y., 2000, *Bull. Chem. Soc. Jpn.*, **73**, 2461.

[25] Kozuka, T., Sakai, T., Miyamura, R., and Kawahara, M., 2003, *ISIJ International*, **43**, 884.

[26] Uechi, I., Katsuki, A., Dunin-Barkovskiy, L., and Tanimoto, Y., 2004, *J. Phys. Chem. B*., **108**, 2527.

[27] Duan, W., Kitamura, S., Uechi, I., Katsuki, A., and Tanimoto, Y., 2005, *J. Phys. Chem. B*., **109**, 13445.

[28] Kitazawa, K., Ozeki, S., Tanimoto, Y., and Yamaguchi, M., 2002 *"Jikikagaku"*, IPC, Tokyo; sec. 2.

[29] Atkins, P. W., *Physical Chemistry*, 1990 (Oxford: Oxford University Press) Chp. 25, Chp. 30.

[30] Fahidy, T. Z., 2002, *J. Appl. Electrochem*. **32**, 551.

[31] Chem. Soc. Jpn. Ed., 1996, *KAGAKU BINRAN KISOHEN II 4th edition, Handbook of Chemistry and Physics*, (Tokyo, MARUZEN).

Table 1. All the forces induce by magnetic fields

z / mm	B / T	Field gradient / T^2m^{-1}	F_v / $Nmol^{-1}$		F_L / Nm^{-3}	F_h / Nm^{-3}
			Copper ion	Silver ion	Silver ion	Silver ion
outside	ca. 0	ca. 0	ca. 0	ca. 0	ca. 0	ca. 0
100	4	200	3.14	-0.093	159	-934
135	6	400	6.28	-0.187	238	-2100
170	9	950	14.9	-0.444	358	-4730
200	12	1250	19.6	-0.584	477	-8400
270	15	0	0	0	596	-13100

Figure captions

Fig. 1. Schematics of the experimental set-up of the present experiment in a magnetic field; dark areas are copper plates. The magnetic field direction is applied perpendicularly downward.

Fig. 2. Distribution of the magnetic field B_z and the product of magnetic field intensity and gradient $B_z \times \partial B_z/\partial z$ in the down half part of the bore tube, which was used in the present experiment; z is the distance from the bore tube centre. The broken line represents the product of the magnetic field and the magnetic field gradient. The solid line represents the magnetic field intensity.

Fig. 3. Photographs of silver dendrites after 1 h reaction in set-up (I). (a) Pattern in the outside (ca. 0 T, ca. 0 T^2 m^{-1}). (b) Pattern in the 4 T, 200 T^2 m^{-1} magnetic field. (c) Pattern in the 6 T, 400 T^2 m^{-1} magnetic field. (d) Pattern in the 9 T, 950 T^2 m^{-1} magnetic field. (e) Pattern in the 12 T, 1250 T^2 m^{-1} magnetic field. (f) Pattern in the 15 T, 0 T^2 m^{-1} magnetic field.

Fig. 4. Photographs of silver dendrites after 1.5 h reaction in set-up (II). (a) Pattern in the outside (ca. 0 T, ca. 0 T^2 m^{-1}). (b) Pattern in the 4 T, 200 T^2 m^{-1} magnetic field. (c) Pattern in the 6 T, 400 T^2 m^{-1} magnetic field. (d) Pattern in the 9 T, 950 T^2 m^{-1} magnetic field. (e) Pattern in the 12 T, 1250 T^2 m^{-1} magnetic field. (f) Pattern in the 15 T, 0 T^2 m^{-1} magnetic field.

Fig. 5. Schematic explanation of MHD mechanism and MHD induced trajectories of silver ions. Here, (a) shows the MHD mechanism, where (i) means torque, (ii) means the beamed diffusive flow of silver ions. Also, (b) displays the oriented flow in case of set-up (I), the inner boundary also can also be considered as the inner of set-up (II); (c) displays the oriented flow in case of set-up (II).

Fig. 6. Illustration of convection induced by vertical magnetic force (a) and the Nernst diffusion layer (b). Also, (b) can be considered as the diffusion layer in the present reaction.

Fig. 7. Calculation results of the proportion of $|F_L/F_h|$ with increasing magnetic flux density B.

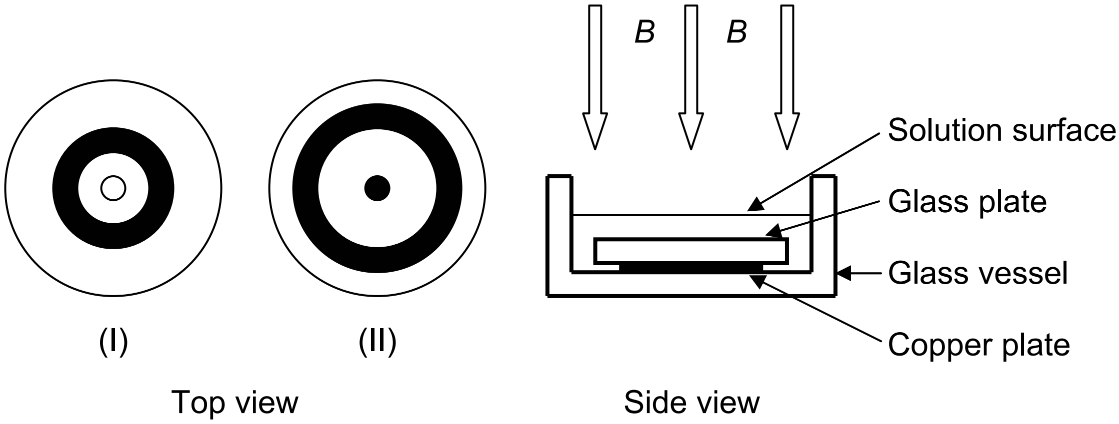

Figure 1 F. Tang et al.

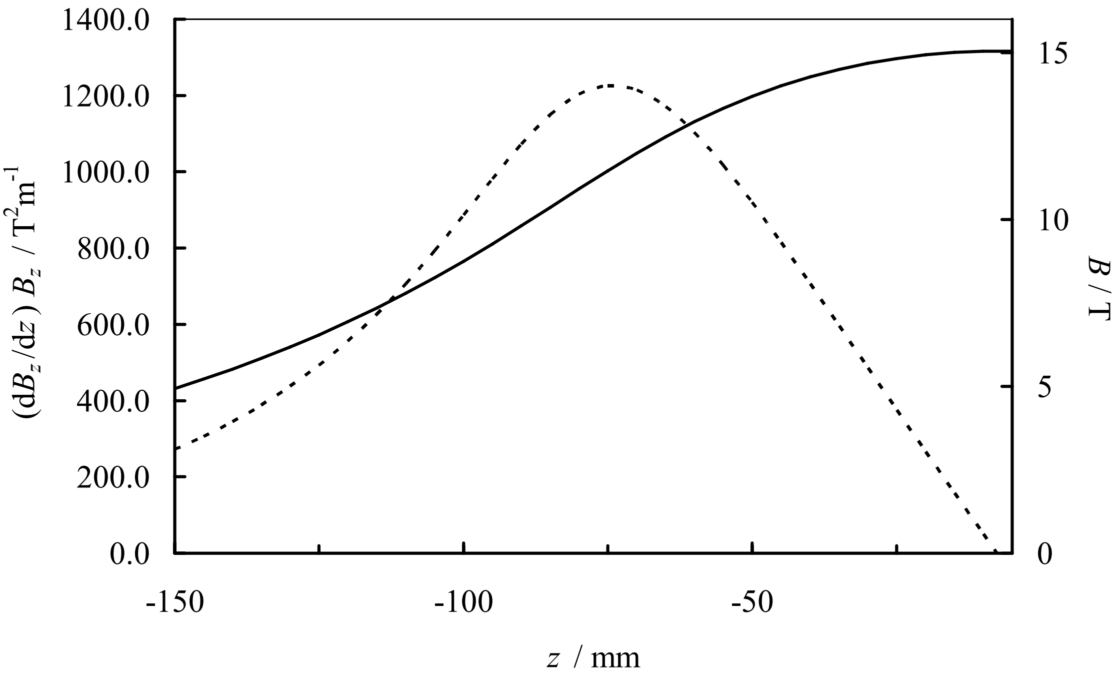

Figure 2 F. Tang et al.

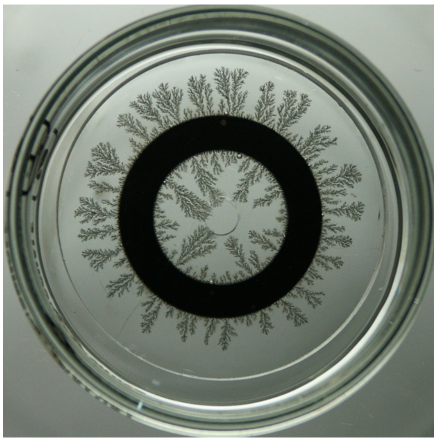
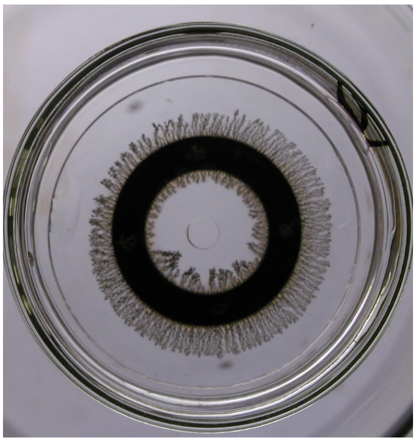
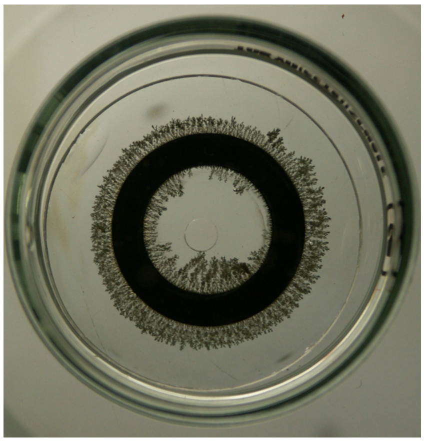

(a) (b) (c)

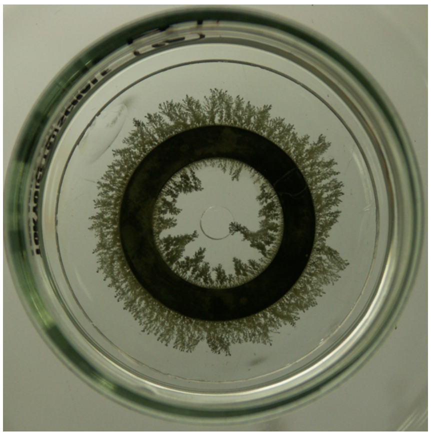
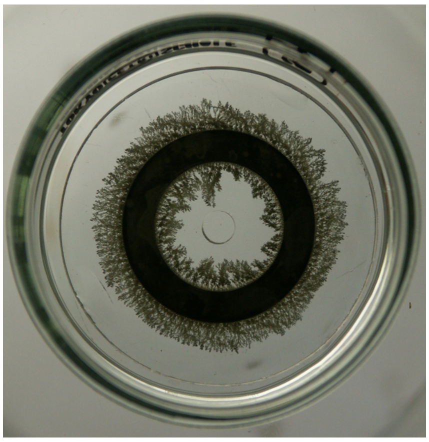
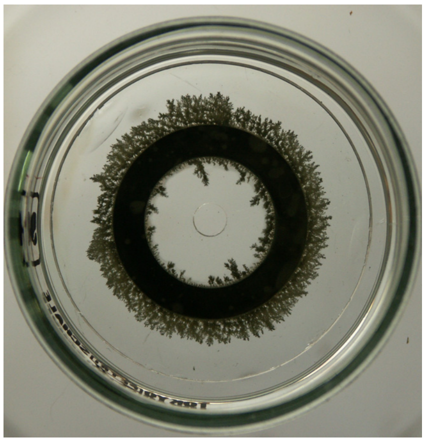

(d) (e) (f)

Figure 3 F. Tang et al.

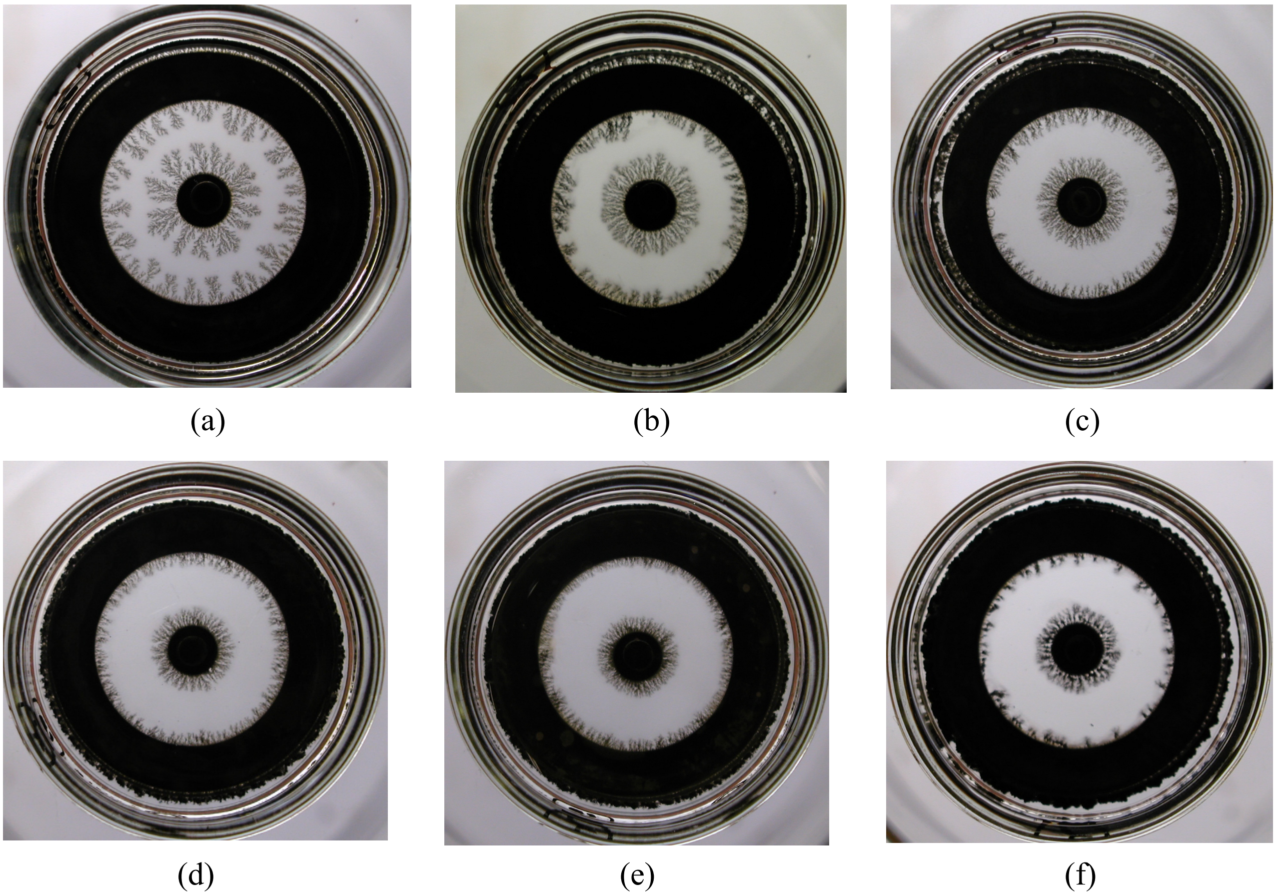

Figure 4 F. Tang et al.

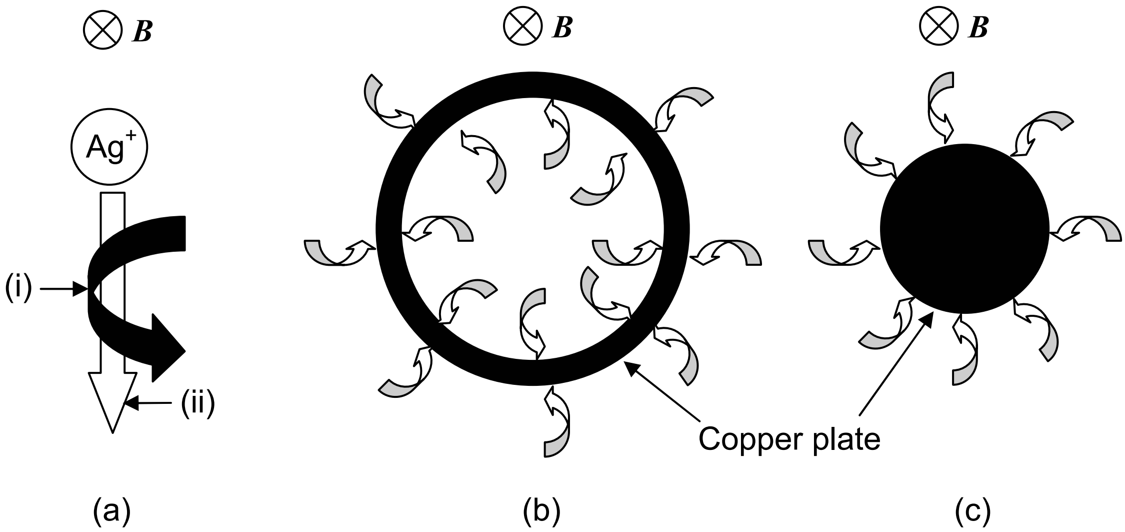

Figure 5 F. Tang et al.

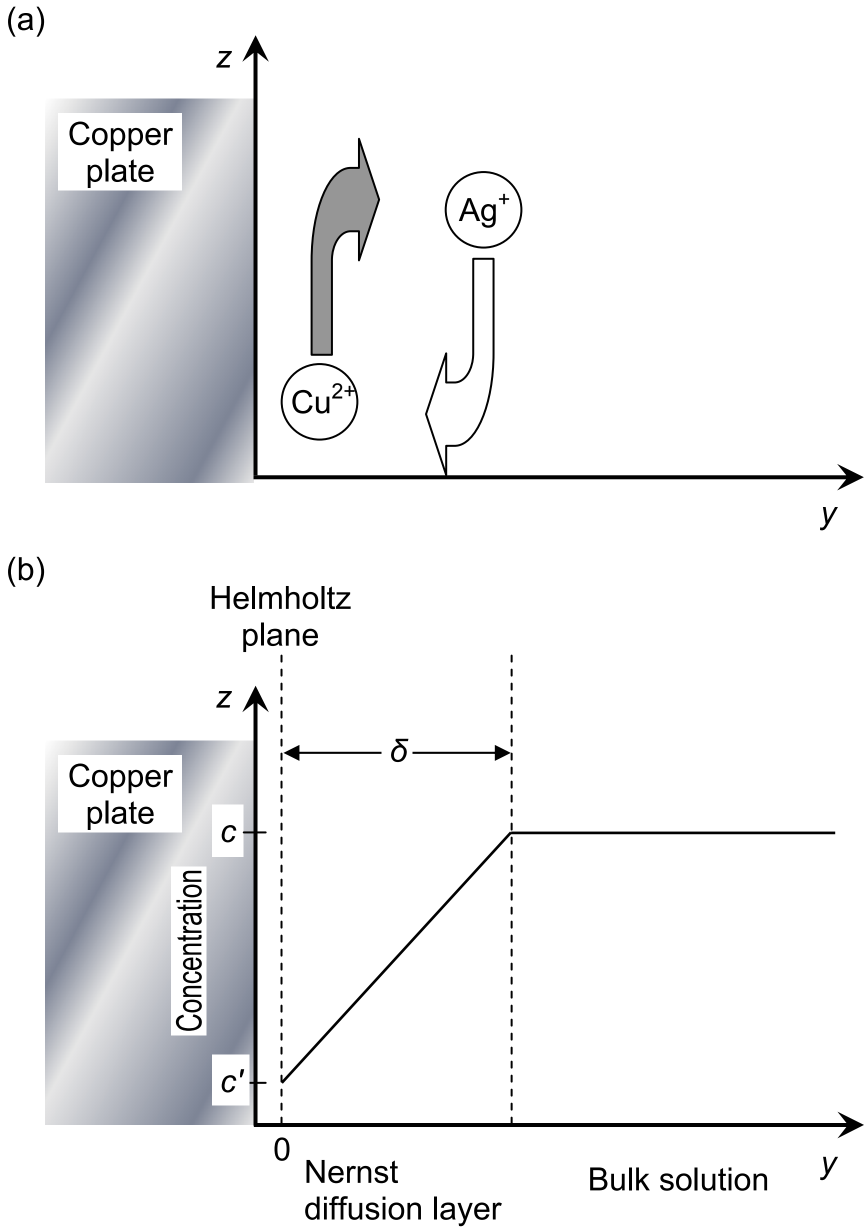

Figure 6 F. Tang et al.

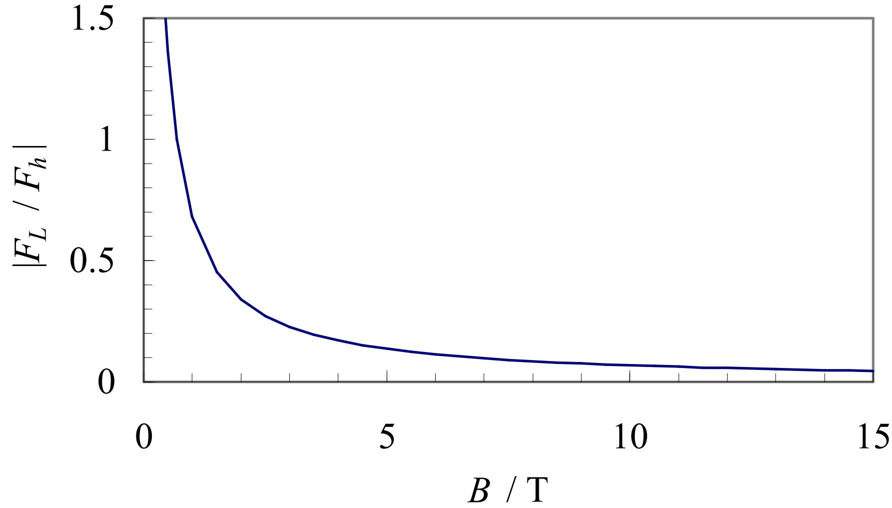

Figure 7 F. Tang et al.